



Research Article

Machinability evaluation of coated carbide inserts in turning of super-duplex stainless steel

Pranay Kumar Parsi¹ · R. Sreeram Kotha¹ · Thomas Routhu¹ · Shashank Pandey¹ · Maheshwar Dwivedy¹ 

Received: 7 January 2020 / Accepted: 22 September 2020 / Published online: 31 October 2020
© Springer Nature Switzerland AG 2020

Abstract

Super-duplex stainless steel (SDSS) is a class of materials that possess excellent mechanical properties with enhanced corrosion resistance. Given the presence of several alloying elements and the existence of a two-phase microstructure, it can be argued that it is one of the few materials that are difficult to machine. Therefore, the present study attempts to establish an improved understanding of the state-of-the-art development in insert coatings capable of providing excellent tribological and thermal resistance properties. In this work, monolayers of AlTiN and AlCrN are PVD coated on commercial carbide inserts so as to compare and contrast the performance of nitride coatings in the dry turning of SDSS. This study evaluates the machining performance in terms of tool wear, chip characteristics, tool life and surface finish. The coated surfaces were observed through optical microscope, profilometers, scanning electron microscope and energy-dispersive X-ray spectroscopy to evaluate the morphological changes. The results of the work indicate that machining with PVD-coated AlTiN insert showed longer tool life, better surface finish and smaller chip thickness when compared to AlCrN-coated and uncoated inserts at low to moderate cutting speeds. The dominant wear mechanism was found to be adhesion, where during turning long continuous chips were formed for uncoated inserts and small segmented chips were formed for coated inserts at different machining parameters. Contrarily, the study also purportedly explores the improved performance of AlCrN-coated inserts over AlTiN-coated inserts at high cutting speed.

Keywords Super-duplex stainless steel · Abrasion · Adhesion · Diffusion · Flank wear · Crater wear · Insert · Coating

1 Introduction

The rising demands from various industrial sectors, including petrochemical, oil and gas exploration; desalination and seawater systems; marine engineering, express the need for materials having superior mechanical performance under scarring environments. The equipment operating under severe corrosive work conditions is exposed to critical operating conditions involving high temperatures and pressures and also exposed to harsh chemicals. Super-duplex stainless steels (SDSS) are a class of materials that

are extremely corrosion resistant and work-hardenable alloys, widely used in applications involving corrosive environment.

Super-duplex steels have brilliant mechanical properties providing both high strength and good corrosion resistance, compared to their cost. These steels combine the characteristics of both ferrite and austenitic steels. The cost factor of SDSS is another reason for its superiority over other material options as it offers to be an economical alternative over nickel alloys, stainless steels, etc. [1]. Therefore, the demand of these steels is rapidly rising

Electronic supplementary material The online version of this article (<https://doi.org/10.1007/s42452-020-03570-9>) contains supplementary material, which is available to authorized users.

✉ Maheshwar Dwivedy, maheshwar.dwivedy@bmu.edu.in | ¹Department of Mechanical Engineering, BML Munjal University, Gurgaon 122413, India.



SN Applied Sciences (2020) 2:1933 | <https://doi.org/10.1007/s42452-020-03570-9>

every year. Due to the versatile properties of super-duplex steels, which include high yield and tensile strength, increased tendency for work hardening and high ductility, the ability to machine these steels is greatly impaired [1–4]. In comparison with austenitic alloys, the life of cutting tool inserts used in machining of these steels is shorter. Cutting forces play a vital role in the quality of the surface produced after the machining, which indirectly gives us the measure of tool wear [5].

Due to the low machinability, various tool wear mechanisms come into action, ultimately causing the reduction in the tool life. Among all wear mechanisms acting, the flank wear has been accounted as the principal mechanism to understand the consequences of tool wear over the surface irregularities of the workpiece [6–9]. It is also the principle criteria for tool life as per the ISO 3685 standard [10]. Alongside the development of new wear-resistant cutting tool materials, there is a growing body of literature that investigates thin-film surface coatings on cutting tools as an alternate to enhance the tool life significantly. This helps improve the production efficiency, reduce processing costs and assure better processed quality.

The physical degradation of cutting tools through tool wear impacts not only the surface texture but also surface integrity leading to lower product quality. As a consequence, the cost of production increases due to increased tooling requirement and undesirable production halts. A number of studies have noted that in general the cutting forces are reliant on the wear rate of cutting tool, and forces increase with the increase in wear. It is reported that cutting tool failure primarily accounts for about 1/5 to 1/3 of the total machine stoppage time [3]. Wear in cutting tools can be broadly classified into two parameters [11]: (i) *mechanical* parameters, abrasion and adhesion, which are affected by thermally loaded contact in between the workpiece and cutting tool; and (ii) *chemical* parameters, oxidation and diffusion, which occur due to the chemical interactions caused by the steep temperature rise [12].

Abrasion wear is caused when grains from the tool's surface break off during the process of turning, creating scratches onto the tool surface as they are restricted in between the workpiece and cutting tool [6, 7, 13–15]. The tendency for the creation of built-up edge (BUE) between the chip and the cutting edge of tool [16, 17] is the major reason for adhesion wear development. Emergence of BUE is periodic, that is, it first grows, becomes wobbly and breaks down, starting the same cycle again. When it shears off, it carries away some particles of the flank surface as well, aggravating the tool wear [18]. This can be attributed to low rake face cutting temperatures. The presence of diffusion wear quickens the other wear mechanisms of abrasion and adhesion [19]. Among all wear types, the most serviceable wear for measuring is wear on the principal

flank [10]. In general, flank wear progression is characterised by rapid initial wear followed by linear growth in the wear and again a rapid rise in the end before the rupture of the cutting tool edge [19]. While wear on the face and side flank could disrupt the geometry of cutting tool, flank wear remains the principal cause of tool failure in majority of the literatures [20]. A single-point cutting tool is considered to have worn out when the maximum land width of flank wear (VB_B max) approaches 0.6 mm for tools with non-regularly worn flank, and average width of flank wear (VB_B) is 0.3 mm for regularly worn tool [10].

In the past few decades, it has been affirmed that thin-film coatings on the surface of cutting tools significantly enhance the machining processes in terms of improved resistance to wear, quality of machining and reduced machining time [21]. These coatings improve the life as well as performance of the cutting tools during high-speed dry machining [22]. With surface coating techniques, only surface properties of the materials are modified where the wear phenomenon occurs, whereas the bulk material remains the same. These coatings provide superior surface hardness, increased wear resistance, reduced frictional coefficients and cutting forces to facilitate chip sliding, greater corrosion and oxidation resistance, and improve the quality of surface finish for machined parts [23]. These benefits are achieved owing to low friction present near the cutting tool–chip interface and high thermal-chemical stability [24].

Hard coating is among the most important process for the cutting tools used in manufacturing industries nowadays [17, 25, 26]. They show the striking diversity of microstructures with regard to the surface morphology as well as phase composition. Among the different hard coatings developed, AlTiN has gained greatest prominence in the recent years owing to its further improved oxidation resistance and hardness. However, AlCrN coatings have been investigated to possess greater oxidation resistance due to the presence of both Cr and Al which can form defensive oxides suppressing oxygen diffusion in comparison with the TiN-based coatings. The wear behaviour of differently coated cutting inserts, such as TiCN, TiCN + TiAlN, TiAlN, Al_2O_3 + TiCN, has been thoroughly examined in the machining of tool steel [27]. The study reports that cutting tools coated with TiAlN performed better, attributing to their greater high-temperature stability. A decrease in cutting forces was observed while turning stainless steel using CA-PVD TiN-coated cutting tools [28]. Similar observations were also reported in dry machining of 0.5–0.6% carbon steel with carbide inserts coated with PVD TiN [29] where a significant reduction in cutting forces was achieved in coated tools over uncoated cutting tools. In the machining of tool steels with TiN-coated CBN tools [12], abrasion wear is the dominant wear mechanism at

low operating conditions, while at high cutting speed the presence of adhesion wear results in BuE formation on the cutting tool which is reported to be responsible for reducing the tool wear rate.

While machining of SDSS with PVD- and CVD-coated cutting tools, PVD-coated cutting tools performed better with the least wear volume in contrast with CVD-coated and uncoated cutting tool [4]. The reason for this was attributed to the formation of tribo-films. During dry turning of 0.4% C steel by CA-PVD TiN-coated carbide cutting tools [30], flank wear was reportedly found to decrease by a whopping 30%. During the inspection of the microstructures of both single- and dual-layer coatings of AlCrN, TiAlN, and AlCrN/TiAlN using plasma-assisted PVD [31], AlCrN coating was observed to be consistent and extremely dense, containing limited micro-voids when compared to AlTiN coating which was non-uniform and porous. AlCrN coating possess good adhesion to substrate and better chemical stability at elevated temperatures [32].

The superior properties of SDSS can be attributed to their biphasic microstructure combining the positives of both ferritic and austenitic stainless steel with proper balancing (*near equal volume percentages*) [13]. The grain size and the lamellae distance between the ferrite and austenite phase have strong influence on their strength [33]. The duplex structure also strengthens their performance, toughness and ductility; as a result, these steels have a pitting resistance equivalent (PRE) index greater than 40 (based on 24% Cr + 3.3% Mo) [34]. The combination of Cr, Mo, Cu, Si and W in these steels influences structural equilibrium and provide better corrosion resistance [1].

Although their characteristics suit well for a variety of industrial application, superior mechanical properties, in turn, negatively affect the machinability of SDSS. Due to high yield and tensile strength as well as higher rate of hardening, machining of super-duplex steels gives rise to diverse mechanisms of tool wear like diffusion, abrasion, adhesion and mainly the development of built-up edge (BUE). When cutting speeds are less, BUE formation is stimulated by high ductility causing shorter tool lives in comparison with machining other stainless steels [1]. Alternatively, increasing the speed leads to rise in cutting temperatures which in turn gives significant rise to other wear mechanisms, like diffusion and abrasion. Owing to their superior mechanical properties, heat from the cutting region is not significantly removed and is absorbed by the cutting tool edge. Therefore, high ductility of SDSS causes increased cutting temperatures, development of BUE and consequently, inflated rate of cutting tool wear. This increase in wear results in formation of unstable chips and vibrations, and hence, poor surface finish of the workpiece. Reduced machinability,

with machinability index of around 0.5 as compared to 0.6 of ferritic stainless steels [33], impacts the economics of the process, incurring greater costs to the process relative to other stainless-steel grades.

The literature studied contained the comparison of different Ti-N-based coatings for their machining advantages. Al-Cr-based coatings have also been reported to offer significant improvement in the desired characteristics of the substrate. Although a lot of research has been done to individually analyse the behaviour of AlTiN- and AlCrN-coated inserts, there is no significant comparison of different hard coatings (AlTiN & AlCrN) deposited over the carbide inserts and their characteristic effects on the wear of tool as well as surface roughness of the finished super-duplex stainless steels. Therefore, the current study encompasses the examination of the machinability of AlCrN and AlTiN coatings for their application to carbide cutting tools. The wear of the cutting tool along with the surface roughness of the workpiece for different hard coatings was also determined experimentally. Through this work, effort has been made to develop the optimal strategy for machining of SDSS, analysing the wear characteristics of cutting tools with hard coatings (AlTiN & AlCrN) on cutting tools inserts, along with the optimum levels of surface roughness, aiming for longer tool life and high process productivity.

2 Experimental design (methodology)

2.1 Equipment

2.1.1 Workpiece material

The turning investigations were performed on test specimens (round bar) of SDSS UNS S32750, with dimensions of $\phi 50 \times 100$ mm. This category of stainless steel is considered for industrial applications that involve high mechanical strength along with high corrosion resistance (Tables 1, 2).

Table 3 displays the chemical configuration of SDSS UNS S32750, used in the turning tests, and Table 4 illustrates some of the mechanical characteristics of this grade of steel (Table 5).

Table 1 Mechanical properties of SDSS (UNS S32750)

Ultimate tensile strength	800	MPa (min)
Elongation	15	% (min)
0.2% yield strength	550	MPa (min)

Table 2 Physical properties at room temperature

Thermal conductivity	15	W/m-K
Modulus of elasticity	200	Gpa
Thermal expansion	11	mm/m °C
Specific heat (0–100 °C)	500	J/kg-K
Density	7.8	g/cm ³

Table 3 Chemical composition of different elements in SDSS, in % by weight

Element	C	Cr	Cu	Mn	Mo	N	Ni	P	S	Si
% Weight	0.03 max	24.72	0.5 max	0.69	3.30	0.24–0.32	6.72	0.035 max	0.02 max	0.8 max

Table 4 Mechanical properties of SDSS (Grade S32750) [53]

Proof strength (Mpa)	Ultimate tensile strength (Mpa)	Elongation, min (%)	Hardness (HRC)
550	800–1000	25	32

Table 5 Characteristics of different coating systems

Coating	Coating colour	Hardness (GPA)	Intrinsic stress (GPA)
AlCrN	Light grey	36 ± 3	– 3 ± 1
AlTiN	Grey	35 ± 3	– 3 ± 1

2.1.2 Cutting tools

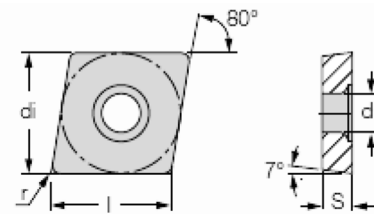
Standard indexable carbide inserts with ISO geometry CNMG-12-04-08, coated with PVD AlCrN and PVD AlTiN, were used for the cutting experiments. The uncoated carbide inserts were supplied by ISCAR. The PVD coatings on the inserts were deposited on tungsten carbide cutting tool using a system bias and CA-PVD at Oerlikon Balzers facility. The coating characteristics of PVD inserts used for cutting experiments are depicted in Table 3. The monolayer PVD-based coating, with a coating thickness of 3–4 μm, offers outstanding resistance with decent adhesion on the shrill edges, higher toughness and better resistance against the formation of crater wear. The dimensions of the insert used in the experiments are depicted in Fig. 1.

The machining experiments were performed on a Batliboi CNC Lathe (in Fig. 2).

The process parameters used for turning based on standard recommendations [3, 17, 21, 35–40] are given in Table 6.

2.2 Experimental method

The CNMG-12-04-08 cutting inserts were synthesised with AlTiN and AlCrN PVD monolayer coatings under special request from Oerlikon Balzers India Pvt. Ltd. The facility involved eight front loading cathodic arc sources, wherein four sources with composition 50at%Ti–50at%Al were used to deposit AlTiN coating, whereas sources with



$$l = 12.90; r = 0.80; di = 12.70; S = 4.76; d_1 = 5.50$$

Fig. 1 Dimensions of turning insert used for experiments [52]



Fig. 2 CNC Turning Centre

70at%Al–30at%Cr were used for AlCrN deposition. The coating thickness over the substrate was determined by the deposition time.

In order to evaluate the microstructure of super-duplex stainless steel, test samples were prepared. These samples were ground on polishing machine using emery papers (220, 320, 400, 600, 800, 1000, 1200, 1500 and 2000, sequentially). Post-grinding, the samples were polished

Table 6 Machining parameters used in the experiments

Machine tool	CNC lathe machine
Workpiece	Super-duplex stainless-steel rod (UNS 32750)
Cutting tool	Coated cemented carbide; CNMG-12-04-08
Depth of cut	2 mm
Feed rate	0.3 mm/rev
Cutting speed	100 m/min, 140 m/min
Frequency of flank wear study	After every two passes

using alumina powder, followed by diamond paste polishing. To reveal the microstructure, the samples which were polished are etched using a stainless-steel etchant of Carpenter 300 Series (8.5gm FeCl₃, 2.4gm CuCl₂, 122 ml ethanol, 122 ml HCl and 6 ml HNO₃) by immersing for several seconds. The microstructure was then studied using a Hitachi SU3500 Scanning Electron Microscope.

The flank wear measurement was taken after every two turning passes to determine the tool life using an optical microscope of 45X magnification. The camera in the microscope was linked to a computer which received the images as shown in Fig. 3. Flank and rake surfaces and the BUE formed were photographed. The insert life standard was kept at the flank wear (VB_{avg}) of 0.3 mm in accordance with ISO 3685 Standard [10]. After the experiments, all the cutting inserts were etched with the help of hydro chloric acid solution to eliminate all adhered material so that the mechanism of tool wear can be examined (Figs. 4, 5).

Orthogonal turning of SDSS with coated and uncoated carbide inserts were performed at different cutting conditions. The chip compression ratio was calculated as per the standard procedure [41], after measurements of cut chip thickness using a digital point micrometre. Following these measurements, the morphological study of the worn regions of cutting tools both coated and uncoated was analysed using Hitachi SU3500 Scanning Electron Microscope equipped with Bruker Xflash 6|30 EDS system. It was

**Fig. 4** Setup for SEM-EDS measurements

required to take away the adhered deposits on cutting tool by etching to observe the mechanisms of wear caused due to machining tests. SEM images before and after etching with HCl depicted the BUE adhered and wear mechanisms on the cutting tool faces.

Sections of the finished workpiece were cut for the SEM analysis to study the surface distortions caused in the course of turning process. The roughness of the surface profile was measured after the first pass and the last pass for every insert during the experiment using Mitutoyo's Surftest SJ-210 Profile roughness module to specify the effect of tool wear over the workpiece surface. The procedure which was adopted for measuring the surface roughness of the profile was in accordance with ISO 1997 standard using Gauss filter. A cut-off wave length of 0.8 mm, with measuring speed of 0.25 mm/s and number of sampling lengths, $N = 5$ was used to measure the roughness. The surface roughness parameter considered for the work was arithmetic mean surface roughness value (R_a). Three roughness measurements were recorded on the workpiece and average reading was considered.

Fig. 3 Vision measuring system along with toolmakers' microscope for tool wear measurement

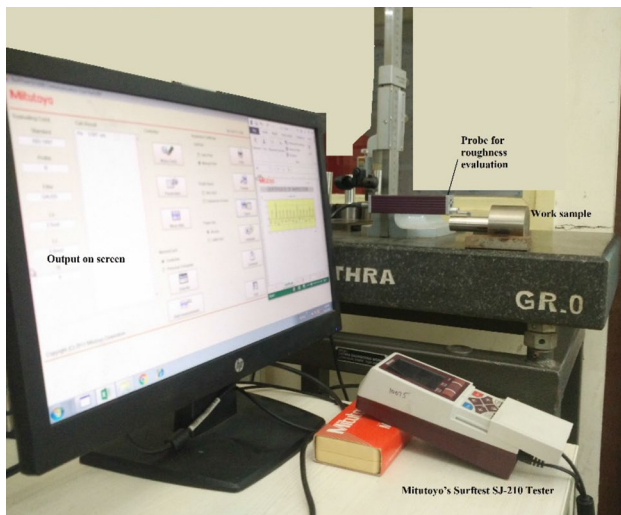


Fig. 5 Mitutoyo's SurfTest SJ-210 Profile roughness module

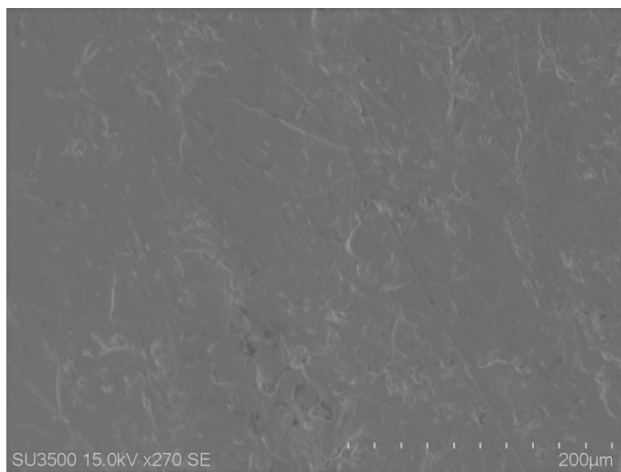


Fig. 6 Duplex microstructure of SDSS at 270 ×

3 Results

To investigate the extent of tool wear (flank as well as crater) on cutting tools with different PVD-coated hard surface coatings (AlCrN and AlTiN) during turning of SDSS, tool wear test was conducted to analyse wear and correlated with surface texture and surface integrity studies.

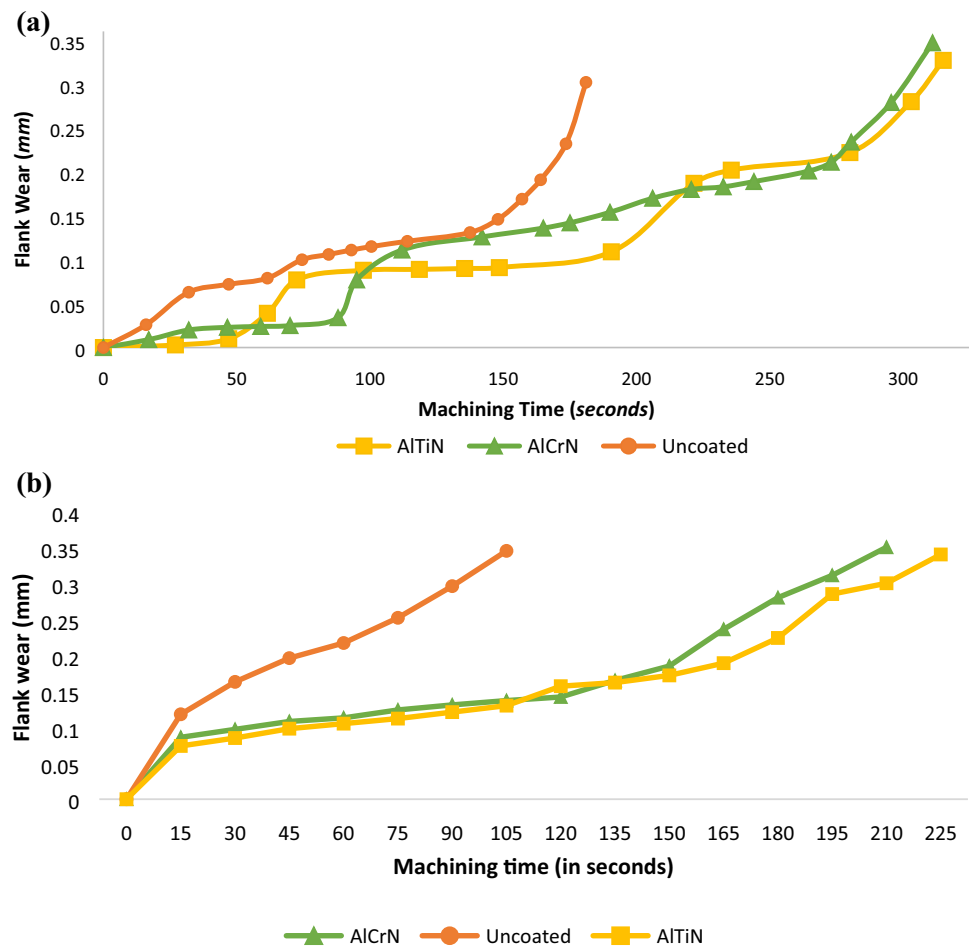
Post-polishing and etching, the microstructure of the SDSS shows the presence of two different Fe-phases as in Fig. 6. The presence of austenite phases in the ferrite matrix confirms the duplex nature of the workpiece.

3.1 Tool life evaluation

Figure 7a illustrates the plot depicting the progression of flank wear along with the cutting time for uncoated, PVD AlTiN-coated and PVD AlCrN-coated cutting inserts during turning of SDSS. It is observed that there is a significant improvement in the wear characteristics when machining with PVD-coated (AlTiN and AlCrN) inserts as compared to uncoated carbide cutting tool insert. It can be seen that the PVD-coated (AlTiN and AlCrN) cutting inserts have a tool life almost twice that of the uncoated insert. Although the tool life of both AlCrN- and AlTiN-coated inserts is comparable with AlTiN marginally better, the wear progression in both inserts is very dissimilar. For AlTiN-coated inserts, there are stages during wear progression where the flank face is stable with increasing machining time, whereas the wear development for AlCrN-coating shows continuous increase in tool wear with the rise in cutting time. This can be accredited to the ability of AlTiN-coated inserts to ameliorate the friction conditions at the interface of cutting tool and workpiece such that smoother chip travel can be achieved over the rake of the cutting tool [4]. This behaviour of AlTiN-coated insert may be attributed to the ability of AlTiN coating to self-organise as a portion of cutting energy during machining is consumed for the self-organisation of coating layer to form lubricating tribo-film that acts as thermal barrier reducing the friction in the cutting zone [42, 43]. However, the flank wear for AlCrN-coated insert shows a continuously increasing trend with machining time because of the presence of greater frictional conditions in the cutting zone, causing significant BUE formation and changing cutting forces as compared to AlTiN. This continuous variation in the flank wear levels for AlCrN coating is detrimental for their industrial utility. The tool life obtained for PVD AlTiN-coated insert confirms that the self-organising behaviour of the AlTiN coating provides better resistance to wear and therefore can be considered as a better alternative with reference to cutting tool life.

Figure 7b represents the flank wear vs machining time for different cutting inserts at 140 m/min cutting speed. At 100 m/min, the inserts had a tool life of 180, 310 and 315 (uncoated, AlCrN coated, AlTiN coated) seconds, whereas at 140 m/min the tool life has been reduced to 105, 210 and 225 (uncoated, AlCrN coated, AlTiN coated) seconds. So, it can be inferred from Fig. 7a, b that as the cutting speed increases, the tool life decreases. The tool life test results at cutting speed of 140 m/min typically follow the same trend as observed at the cutting speed of 100 m/min.

Fig. 7 **a** Development of flank wear for different cutting inserts during machining SDSS at 100 m/min; **b** development of flank wear for different cutting inserts during machining SDSS at 140 m/min



3.2 Wear evaluation at $v = 100$ m/min

The primary objective of this research has been to analyse various mechanisms in which wear is predominant and how this is associated when SDSS is machined by uncoated, AlCrN, AlTiN PVD-coated cutting tools. The wear progression on the crater face and flank of the cutting tool inserts was studied using a Sipcon Vision Instrument System (see Figs. 8, 9). During machining, all the cutting inserts exhibited excessive chipping, adhesion and flank wear, thus resulting in significant reduction in life of the cutting tool. The main reason for this low level of machinability can be attributed to the uncertainty in the formation of chips, along with robust adhesion at the interface of chip and tool, causing BUE, due to high compressive stress. This behaviour can also be attributed to high strain-hardening and low conductivity of SDSS from the presence of alloying elements such as, Cr, Ni and N [21]. Due to the hardening in SDSS, the rise in the frictional conditions between the workpiece and the cutting tool is likely to increase the cutting zone temperature and speed up the tool wear.

The presence of the material from workpiece which is adhered on the rake face of the tool was observed during all cutting experiments using both types of cutting tools (coated and uncoated). The pattern of wear for AlTiN-coated insert (in Figs. 8a, 9a) shows greater incidence for abrasive wear. The rake face for AlTiN does not show significant adhesion of workpiece material, which can be attributed to the low friction conditions present allowing smoother chip flow over the rake face resulting in reduced temperature near the cutting zone and therefore reduced adhesion. For AlCrN-coated insert, Figs. 8b, 9b reveal that there is greater extent of adhesion over the rake face of the cutting tool from the early stages of cutting time itself, as compared to AlTiN-coated insert. This confirms that the self-reorganisation ability of AlTiN coatings helps reduce the adhesion and consequentially crater wear. However, with AlCrN coatings, a significant reduction in abrasive wear over the flank face of the cutting insert was observed confirming better abrasion resistance of AlCrN coating over AlTiN coatings despite similar hardness of both the coatings [44]. This could be attributed to the presence of tribo-film as a result

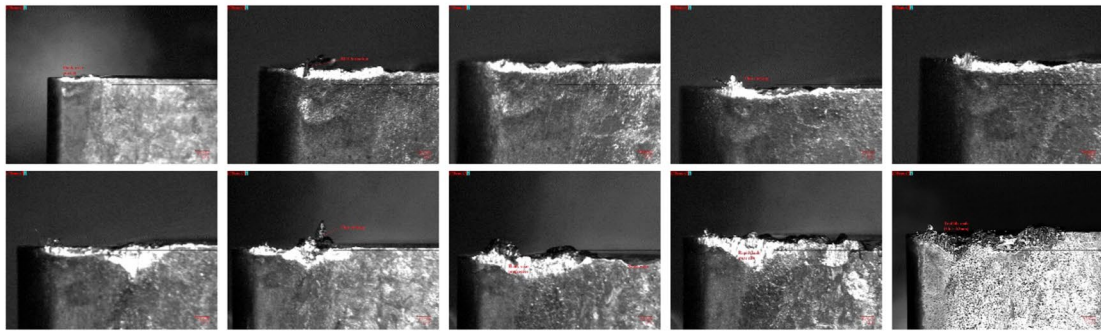
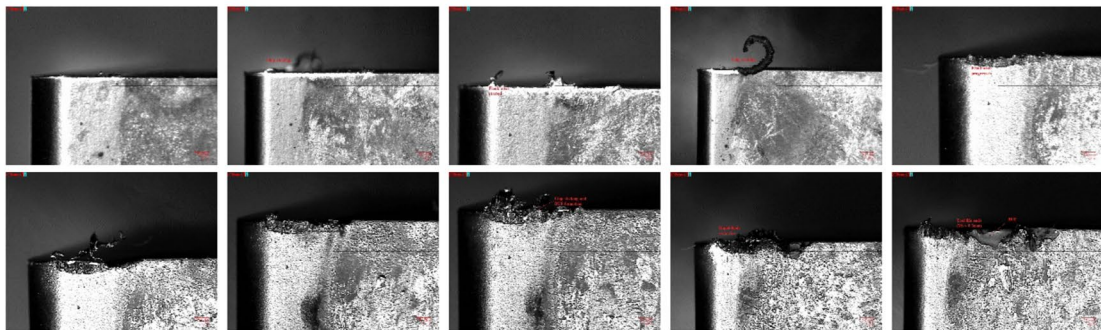
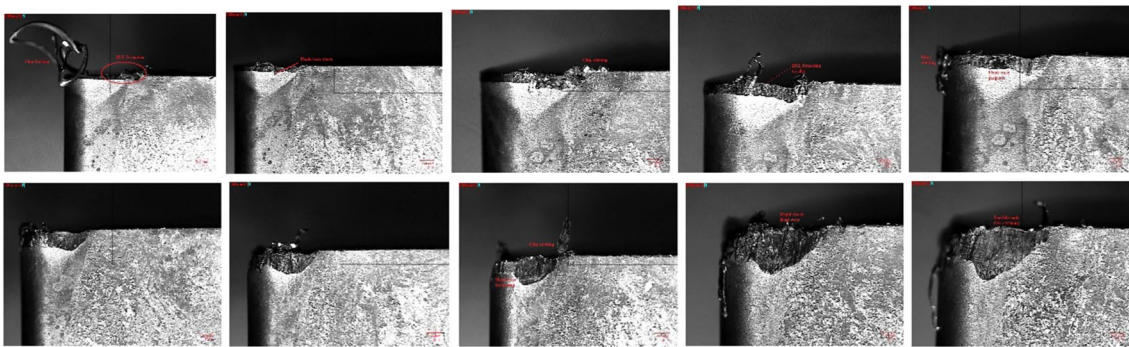
(a) AlTiN**(b) AlCrN****(c) Uncoated**

Fig. 8 Microscopic images showing flank wear progression for **a** AlTiN, **b** AlCrN and **c** uncoated inserts at 100 m/min

of tribo-oxidation forming wear resistant and thermally stable alumina-chromium oxides over AlCrN coating which outperforms AlO_x tribo-film that form over AlTiN coating.

The wear progression for uncoated insert (in Figs. 8c, 9c) shows significant adhesion and abrasion on both the rake and the flank faces of the tool, respectively. Both these wear phenomena were very prominent from the early stages of machining with uncoated carbide inserts. This behaviour of uncoated insert confirms the utility of the

PVD coatings (AlCrN & AlTiN) because of the development of protective oxide layers over the tool's surface.

While machining super-duplex steels, we can observe from Figs. 8, 9 that adhesion and abrasion are the dominant wear mechanisms leading to chipping and flank wear. It has been reported from past studies that adhesion is the primary type of wear which is predominant at lower cutting speeds, whereas failure occurs due to abrasion and diffusion when the cutting speeds are high [15, 45]. To further analyse tool wear, SEM images of worn-out cutting

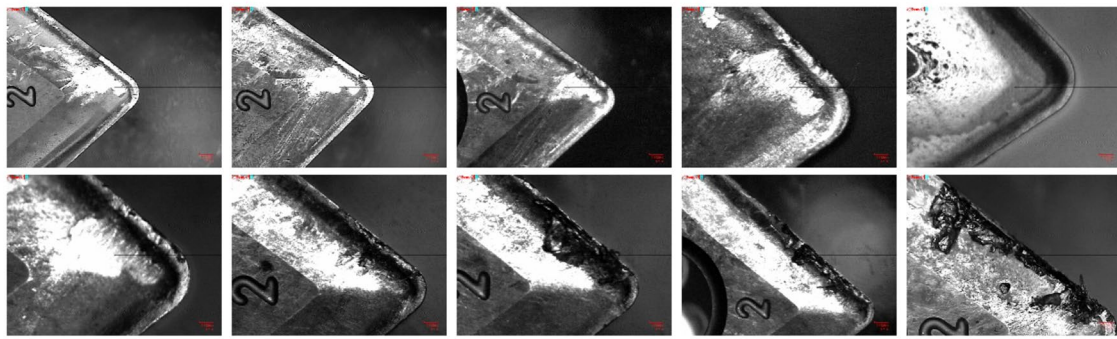
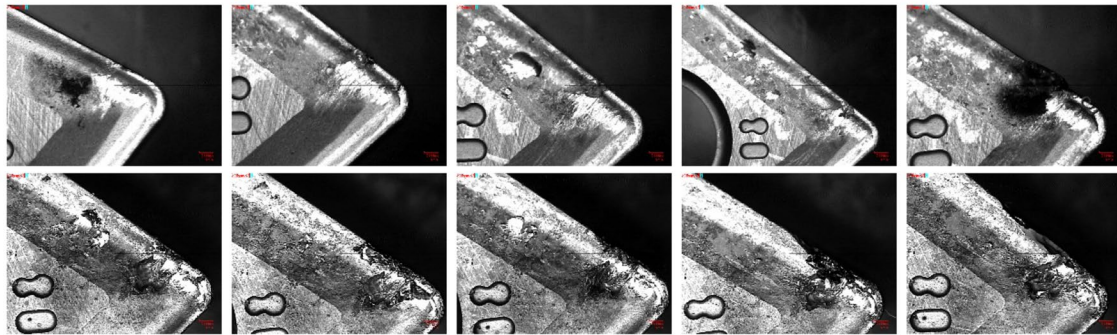
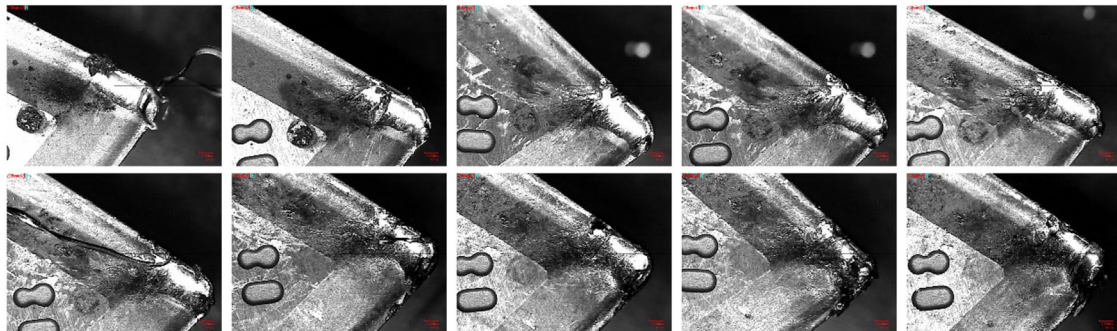
(a) AlTiN**(b) AlCrN****(c) Uncoated**

Fig. 9 Microscopic images showing crater wear progression for **a** AlTiN, **b** AlCrN and **c** uncoated inserts at 100 m/min

inserts at high magnifications before and after etching with HCl were compared to gain further understanding of the underlying wear mechanism. The associated EDS analysis is summarised in Table 7. Post-etching, the EDS results reveal that there is no BUE left adhered to the cutting tool surface, allowing us to distinguish between diverse wear mechanisms acting on the cutting inserts.

Figure 10 displays different wear mechanisms acting on PVD AlTiN-coated cutting insert in detail. Of particular interest is that (see Fig. 10a) the worn-out insert prior to etching shows remnants of workpiece material adhering on the insert rake face. This was confirmed with the help

of EDS-1 where high concentration of iron and chromium indicates the presence of SDSS. The presence of layers of aluminium and titanium oxides can also be noticed over the tool's rake face which reduces the wear, which is confirmed by results from EDS-2 showing significant concentration of oxygen, aluminium and titanium. Figure 10b, e depicts various tool wear mechanisms post-etching after the removal of the adhered work material from the cutting insert, confirmed via EDS-3 and EDS-4. The observed surface alterations on the insert face and flank due to adherence wear while machining SDSS may be partly due to high cutting speed (100 m/min) resulting in high

Table 7 EDS results for worn cutting inserts in Figs. 10, 11, 12

EDS	Chemical composition (%)								
	Fe	W	O	Cr	Ni	C	Ti	N	Al
1	38.92	–	–	16.07	3.65	14.7	–	–	–
2	19.86	–	29.27	8.13	1.65	9.48	9.28	10.78	8.5
3	7.97	47.64	7.11	4.2	0.97	9.52	–	–	–
4	0.64	–	15.77	1.9	–	4.11	37.75	20.47	32.08
5	41.56	–	5.21	17.17	–	16.8	–	–	0.47
6	12.74	47.48	1.99	6.96	–	4.46	–	–	–
7	11.09	–	21.51	32.62	–	4.8	–	2.13	7.14
8	36.69	–	16.42	14.77	–	20.19	–	–	0.87
9	19.64	38.88	1.35	9.18	1.84	7	–	–	–

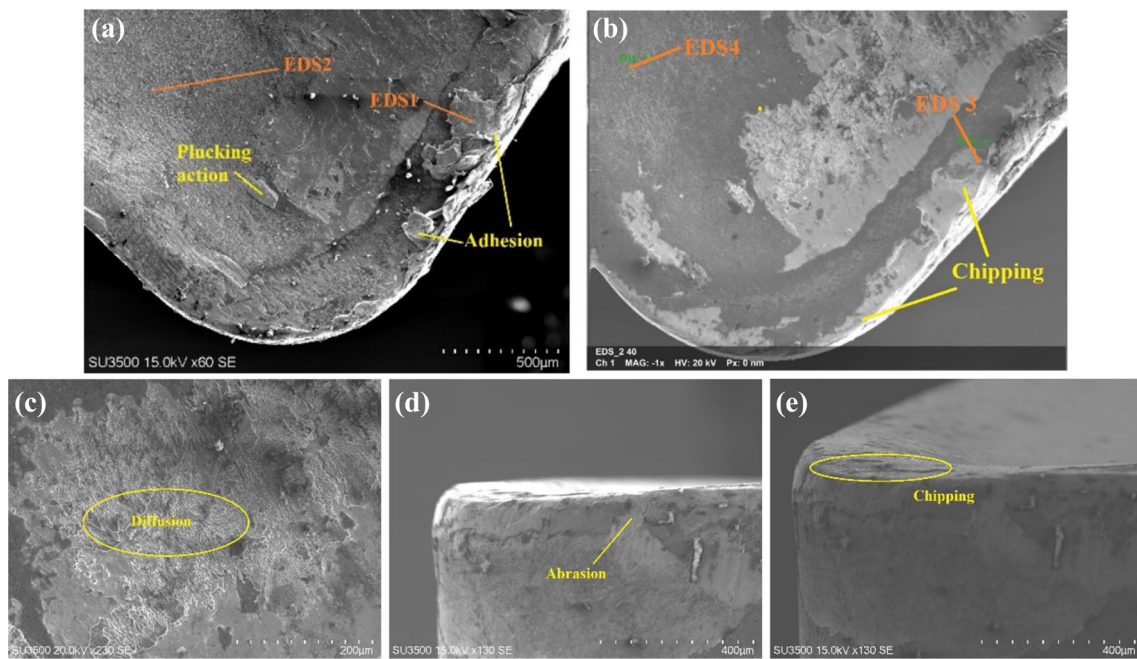


Fig. 10 SEM images of PVD AlTiN-coated insert: **a** insert before etching; **b** insert post-etching; **c–e** different views for wear/distortions

temperature at the affiliate between the tool and the chip. Such plucking action present over the rake face is a result of the plastic flow of material from workpiece [45, 46].

In Fig. 10c, the smooth surface can be attributed to the wear caused due to diffusion. In diffusion wear mechanism, the atoms from the high-concentration (cutting tool) zone diffuse into the low-concentration (chip) zone due to concentration gradient [41]. This phenomenon is dependent upon several factors while machining, cutting temperature, solubility of elements in the secondary shear zone and contact time between workpiece-tool. Diffusion in most cases is restricted to a thin zone at the tool–chip interface; thus, it results in the wearing of the

tool [4]. Figure 10d displays parallel lines in the tool sliding direction against the workpiece, which signifies the presence of abrasive wear. The ASTM standards describe the occurrence of abrasion due to the grinding action of hard particles forced against to move along a solid surface [47], which in this case is the presence of BUE as the hardened substance. Figure 10e displays chipping developed at the tool’s cutting edge indicating that the mechanical fatigue caused by the BUE formation results in cutting tool wear [48].

Figure 11 displays different mechanisms of tool wear for PVD AlCrN-coated cutting insert. Figure 11a depicts the state of cutting tool before etching with HCl showing

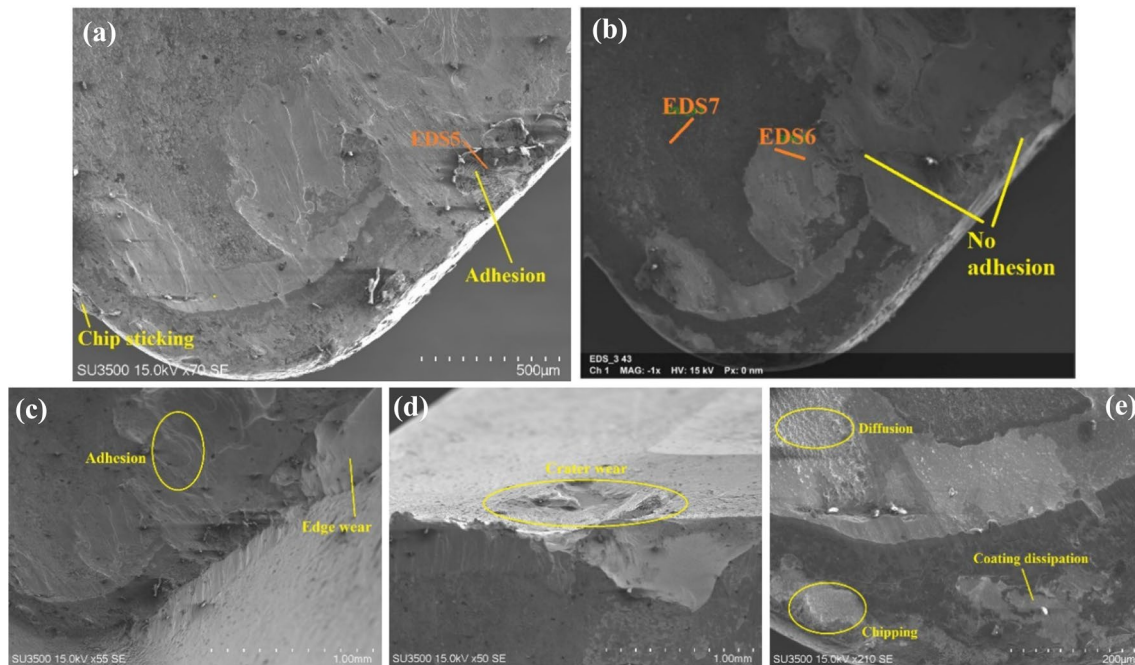


Fig. 11 SEM images of PVD AlCrN-coated insert: **a** insert before etching; **b** insert post-etching; **c–e** different views for wear/distortions

significant chip sticking. EDS-5 confirms the adhesion of workpiece over tool's surface which is indicated by the presence of high concentrations of Fe and Cr. Figure 11b shows the cutting inserts rake face post-etching, as depicted in the EDS-6 and EDS-7 in Table 7, confirming the removal of SDSS (EDS-6) and the presence of AlCrN coating (EDS-7). Figure 11c outlines regions having irregular feature on the tool's cutting edge causing edge wear, which is a distinctive mechanism of adhesive wear [49]. Figure 11d shows significant crater wear on the tool's rake surface caused due to greater levels of adhesion. Adhesive wear often occurs due to the chemical affinity between the workpiece material and cutting tool, ensuing in BUE formation at the insert–chip interface. Figure 11e, at high magnification, illustrates the rake face where the coating is dissipated due to consistent tool wear. Smooth surface suggesting the diffusion wear mechanism was also observed on the tool's rake surface. Chipping can also be seen close to the tool's cutting edge as in Fig. 11e, indicating the increase in thermal load during machining caused due to greater levels of friction offered to chip flow as compared to AlTiN coatings.

Figure 12 displays the mechanisms of wear for uncoated cutting insert. Figure 12a shows the insert before etching, and Fig. 12b–d depicts the wear mechanisms post-etching. Figure 12a displays the cutting tool prior to chemical etching with HCl where BUE and chips are seen to be adhered

on the tool's surface, as confirmed in EDS-8. Figure 12b reveals the severe chipping on the cutting edge post-etching, which confirms the deletion of the adhered workpiece material over tool's rake face. Further, the existence of parallel lines in the tool sliding direction against the workpiece (principal flank) as the underlying mechanism of flank wear is confirmed in Fig. 12c. Figure 12d displays the flank surface of the cutting insert post-chemical etching, indicating regular flank wear. The uncoated tool–work material interface shows high flank and crater wear both as a result of one or amalgamation of the different wear mechanisms [18]. The formation of BUE during the process of machining causes dislocations throughout the cutting process and breaks the cutting edge [14].

In summary, after turning super-duplex stainless steels with different cutting inserts, it can be observed that these tools are greatly affected during machining causing severe tool wear, affirming the low machinability of super-duplex stainless steels. Therefore, in order to attain decent outcomes, it is vital to recognise the cutting insert behaviour during the machining operations. Under the experimental setting, the coated and uncoated inserts displayed wear exhibiting different mechanisms: adhesion, abrasion and diffusion. To ensure better industry utilisation of super-duplex steels, it is crucial to comprehend the causes of these wear mechanisms to mitigate their impact on the tool life.

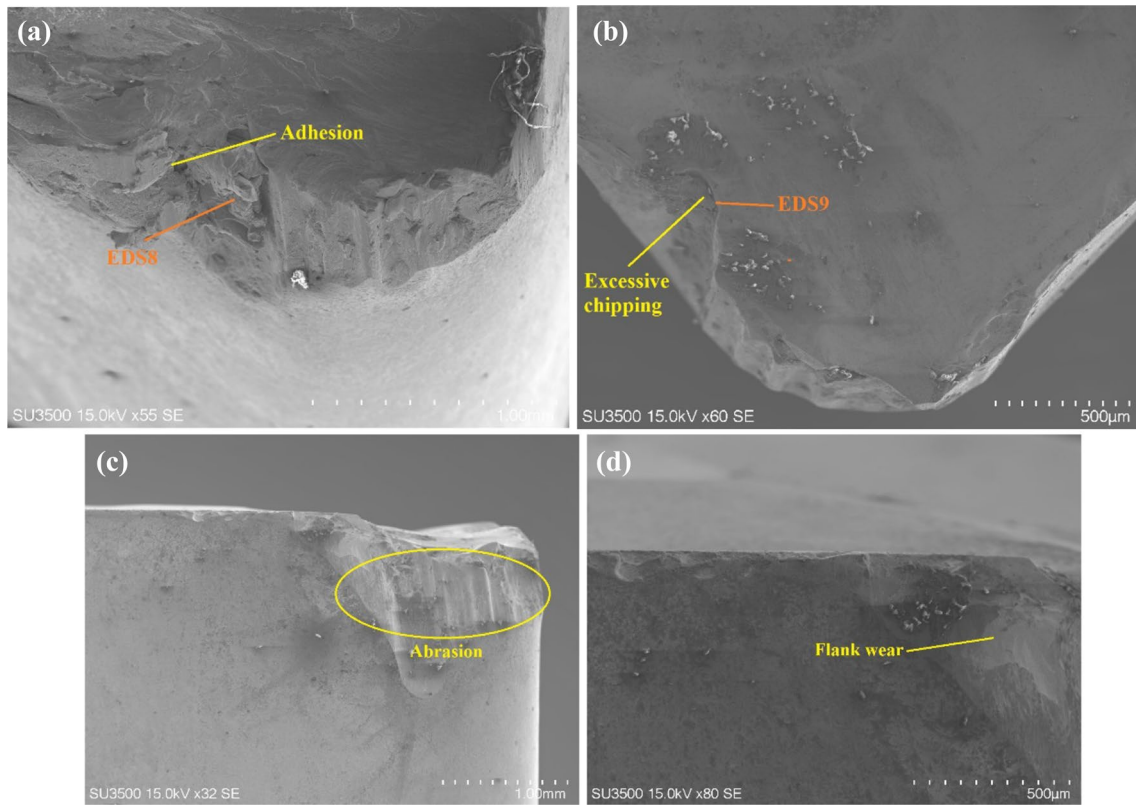


Fig. 12 SEM images of uncoated insert: **a** insert before etching; **b** insert post-etching; **c, d** different views for wear/distortions

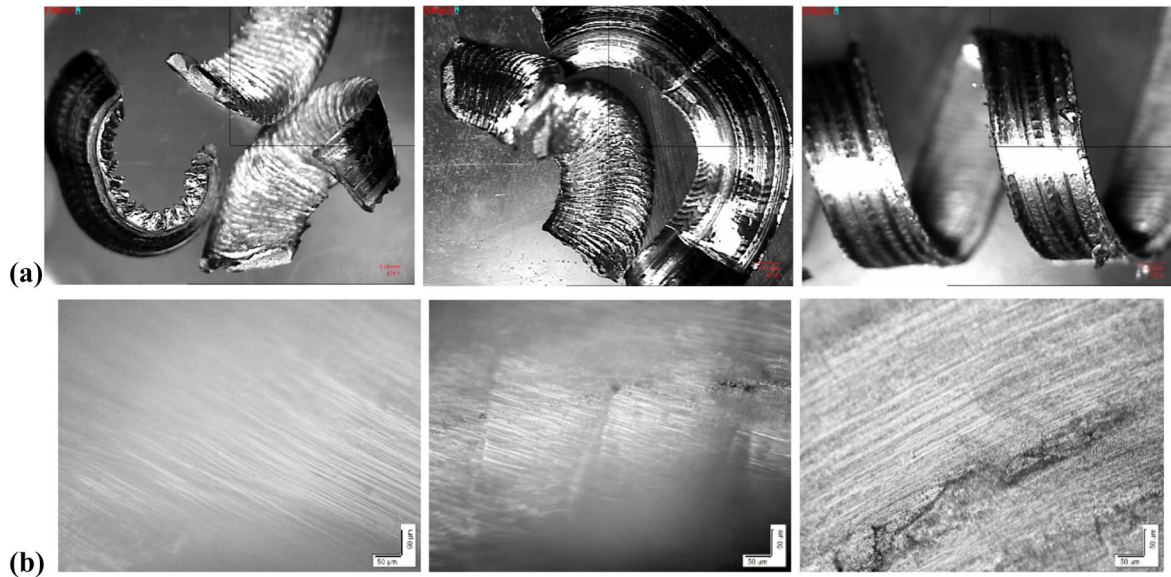


Fig. 13 **a** General macrograph of chips; **b** chip undersurface obtained with (i) AlTiN, (ii) AlCrN and (iii) uncoated inserts

3.2.1 Chip characteristics

After analysing the tool wear, chips morphology was determined for each cutting insert. Macroscopic and

microscopic images of the chips for the PVD-coated (AlCrN and AlTiN) and uncoated cutting inserts are shown in Fig. 13a, b. The macrograph results shown in Fig. 13a indicate the formation of short and segmented chips for

PVD-coated inserts, both AlCrN and AlTiN. The formation of segmented chips ensures minimal interference of chips with the cutting process resulting in smoother flow of chips. However, for uncoated insert, the chips formed are long and continuous in nature. This is in line with the higher wear rate for uncoated tools with the presence of high levels of friction near the tool–chip interface.

The optical micrograph results in Fig. 13b show that the chip undersurface morphology for PVD AlTiN-coated insert is better than AlCrN-coated insert, with uncoated insert producing the poorest chip under surface. The friction conditions for AlCrN-coated insert at the cutting tool–chip interface are high due to which the contact area between the insert and chip on the tool's rake face is increased, causing a varied increase in the machining zone temperature. This rise in temperature because of increased friction also hampers the tool life for PVD AlCrN-coated inserts. The ability of self-organisation for AlTiN coatings provides smoother flow of chips because of the presence of reduced friction conditions and therefore offers better chip undersurface morphology than those observed with AlCrN-coated inserts. The morphology of chip undersurface obtained for uncoated insert shows even greater distortions and cracks owing to even higher levels of frictional conditions present at the interface of tool–chip due to recurring formation of BUE and greater adhesion.

Chip reduction coefficient (ζ) is widely considered as an index of machinability. It can be defined as the ratio of chip thickness to the undeformed chip thickness. The greater value of ζ indicates more chip thickness and hence greater would be the energy required for machining. The extent of chip thickening can be expressed as:

$$\zeta = \frac{a_2}{a_1} \quad (1)$$

where a_2 is the chip thickness, $a_1 (s_0 \sin \varphi)$ is the undeformed chip thickness, s_0 is the feed in mm/rev, and $\varphi (= 90^\circ)$ is the principal cutting edge angle.

Chip samples were collected after each experimental trial at the end of two pass and chip thickness measured. The average values of chip thickness and chip reduction coefficient are tabulated (see Table 8). The chip

characteristic studies in Table 8 revealed that machining with coated cutting inserts produced thinner chips as compared to that of uncoated inserts. This reduction in chip thickness yields lower cutting forces that is required for the shearing action of chips from the workpiece and improves the breakability of chips during machining [50]. The results confirm that the PVD coatings of both AlCrN and AlTiN offer significant advantage to the machining quality when compared to the finished quality attained by machining with uncoated carbide insert. One possible account of the experimental outcome of the improved chip characteristics caused due to improved metal flow for PVD AlTiN-coated insert and PVD AlCrN-coated insert against uncoated cutting inserts is the growth of the tribo-films over the rake face. Al-Ti oxides for AlTiN coating and strong Al-Cr oxides for AlCrN coatings form protective layers over the tool surface and therefore prevent further degradation of the cutting tool. However, the slightly better characteristics for AlTiN versus AlCrN can be attributed to the heat flow distribution taking place for AlTiN coating due to the tribo-films generated during machining. This helps in more efficient dissipation of heat generated during machining through chip removal. These films also improve the frictional performance of the inserts, consequentially providing better wear resistance and smoother chip undersurface morphology.

The continuous and curling chips of SDSS predominantly show a serrated pattern. The machinability index based on chip reduction coefficient value is the lowest for AlTiN-coated inserts and maximum for uncoated carbide inserts. This along with an improved chip under surface makes AlTiN a better alternative over AlCrN-coated inserts at 100 m/min cutting speed.

3.2.2 Machined surface evaluation

The results of the surface roughness tests are summarised in Table 9, and these represent the mean value of three experiments. The results show that the machined surface of the workpiece with coated inserts has lower surface roughness than that of the workpiece machined with uncoated inserts. This can be credited to the lower frictional conditions in the cutting zone of the coated inserts

Table 8 Chip characteristics during turning of SDSS

Type of coating	Chip thickness (mm)	Chip reduction coefficient (ζ)
AlTiN	0.573	1.918
AlCrN	0.667	2.231
Uncoated	0.847	2.833

Table 9 Surface roughness values (Ra) for the machined surface obtained by different cutting inserts

Insert type	After first pass	After last pass
Uncoated	3.192	3.588
AlCrN coated	2.761	3.114
AlTiN coated	2.613	3.047

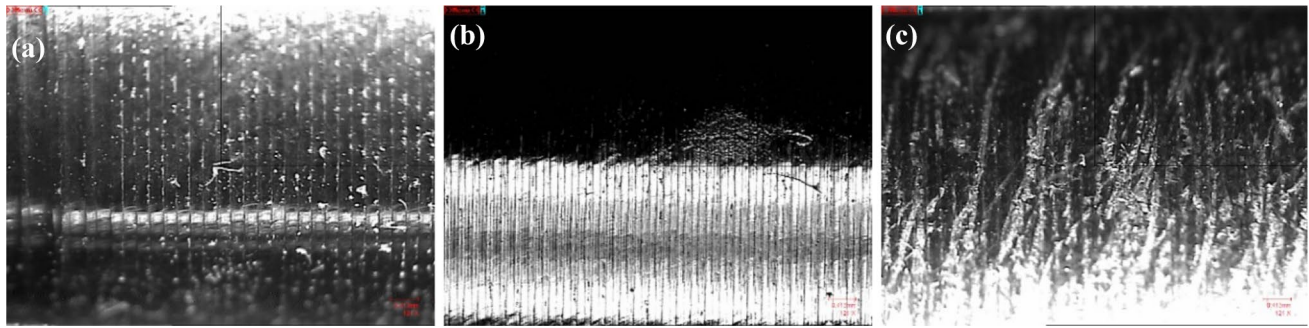


Fig. 14 Microscopic images of the machined surface obtained by **a** PVD AlTiN, **b** PVD AlCrN, and **c** uncoated insert

which resulted in small variation in the cutting forces when compared to the uncoated inserts [4].

The microscopic images for workpieces machined with AlTiN- and AlCrN-coated cutting inserts (in Fig. 14a, b) show smoother finish as compared to uncoated inserts. In Fig. 14c, the machined surface obtained for uncoated cutting tools illustrates cracks and surface distortions. The poor surface finished observed can be attributed to the chip sticking and greater levels of friction produced during machining with uncoated inserts.

The roughness values and their respective evaluation profiles for the finished workpiece machined with uncoated, AlTiN-coated and AlCrN-coated cutting tools are depicted in the graphs in Fig. 15. The results indicate that the surface irregularities are significantly reduced for machining operations with PVD-coated carbide inserts. The evaluation profile for uncoated inserts shows significant degradation in the surface profile from the first pass and the final pass with the same insert.

3.3 Wear evaluation at $v = 140$ m/min

The microscopic images showing the flank and crater wear at 140 m/min cutting speed are given in Figs. 16 and 17, respectively. For each coating type, images after first, middle and last cut are shown. It is clearly evident from the microscopic images that the flank wear pattern for AlTiN and AlCrN is quite similar, with AlTiN showing a much better evolution of flank wear with time. However, the assessment of crater wear confirms that AlCrN is more stable at higher cutting speed as compared to AlTiN as they offer higher abrasion resistance. The characteristic wear observed in AlTiN-coated inserts is edge wear. Significant crater wear leading

to edge chipping is observed in uncoated carbide inserts. The tendency of BuE formation is predominantly noticed in uncoated carbide inserts followed by AlTiN-coated inserts. The cyclic tendency of chip adhering to the tool and breaking off causes adhesion wear in uncoated inserts bringing about frequent changes in the insert angles and hence vibration in the system. This explains the massive edge wear observed in uncoated carbide inserts.

4 Conclusions

Tool life studies are critical for the assessment of productivity. A promising insert coating is expected to wear out progressively with time and behave predictably. The current experimental findings establish the superiority in the performance of coated carbide inserts. Invariably, the tool life of PVD-coated AlCrN and AlTiN inserts was found to be about two times that of the uncoated inserts. Our study clearly indicates the formation of Al–Cr oxides on AlCrN-coated inserts and equivalently Al–Ti oxides on AlTiN-coated inserts. The dominant behaviour of these tribo-oxides confirmed the greater resistance to abrasion of AlCrN coatings as compared to AlTiN coatings. However, the chemical affinity of AlCrN with Cr present in SDSS promotes adhesive wear resulting in wear of the cutting edge leading to significant crater wear. This can be attributed to the formation of BuE at chip–insert interface leading to poor surface finish as observed in our study. The crater wear leads to chipping at the cutting edge, eventually promoting notch wear resulting in exposure of substrate thereby accelerating the process of flank wear with time.

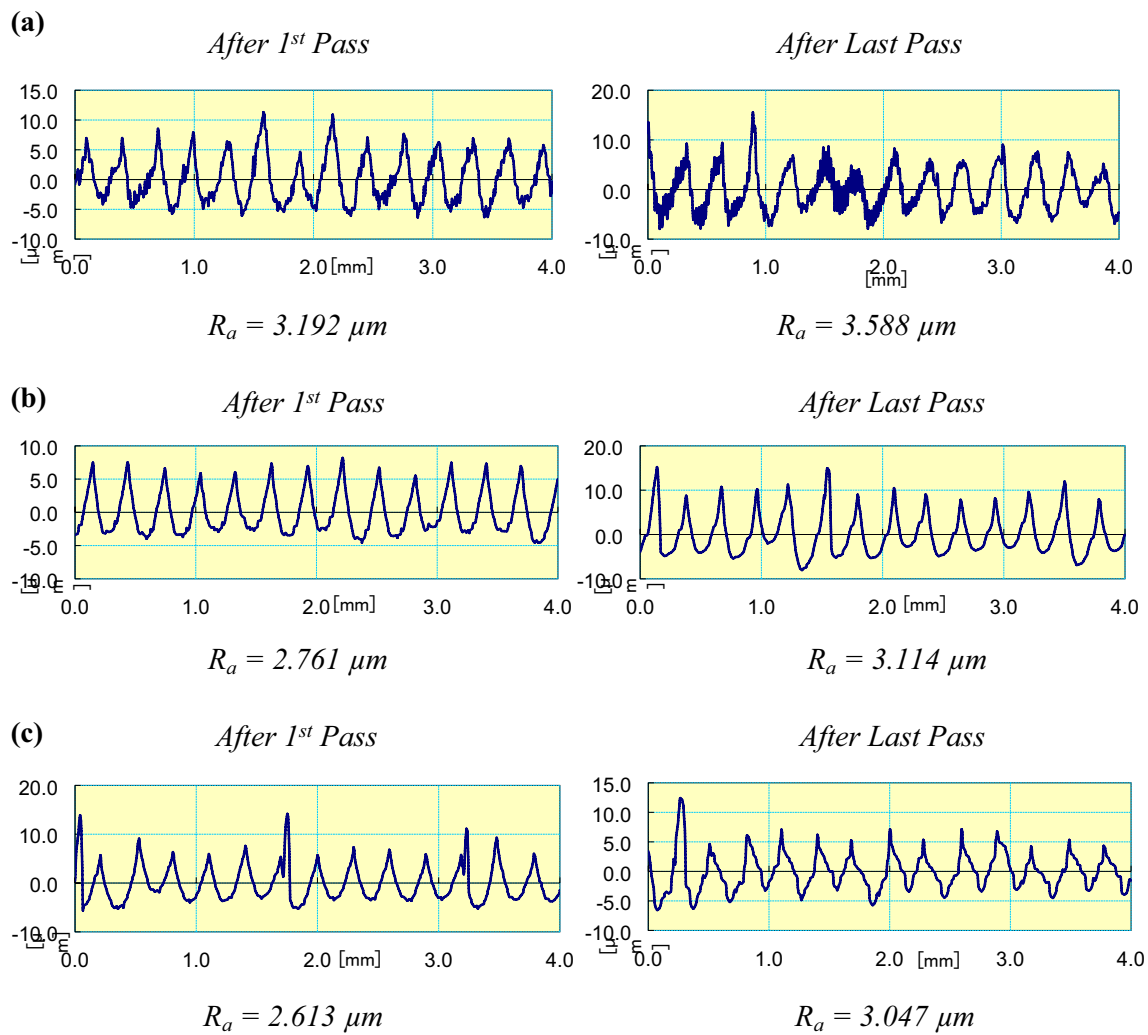


Fig. 15 Surface roughness evaluation curves and corresponding R_a values achieved for machining with new and worn out: **a** uncoated, **b** AlCrN-coated and **c** AlTiN-coated insert

At cutting speed of 100 m/min, our study categorically confirms that adhesion and abrasion are the dominant wear mechanisms leading to chipping and flank wear. So, while AlCrN provides excellent abrasion resistance at $v = 100$ m/min, the prominent presence of adhesive wear right from the onset of cutting time results in the unsatisfactory evolution of its flank wear with time. Contrarily, AlTiN-coated inserts contain Ti which reportedly reduces the chemical reactivity of the coatings and hence less tendency towards adhesive wear. But with shallow depth of cut, as is seen in this study and low to moderate cutting speeds, AlCrN coating would in all likelihood generate high friction due to Al-Cr oxides and also because

of poor thermal conductivity of these oxides, the heat dissipation into the substrate is prevented forcing the heat back into the cutting zone which in turn leads to residual stresses on the SDSS workpiece surface. Our study indicates that AlTiN-coated insert shows superior chip characteristics with more uniform chip undersurface morphology than AlCrN-coated insert, signifying the lesser friction present near the cutting zone which allows the flow of chips over the rake face smoothly. On the contrary, titanium tribo-oxides formed from AlTiN coating have relatively higher thermal conductivity, hence expected to exhibit less residual stresses on SDSS. The surface roughness evaluation for machined

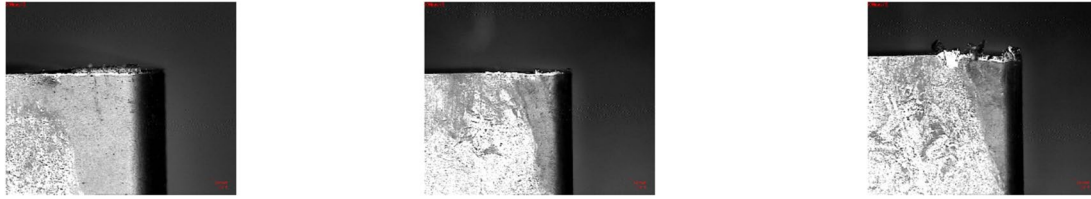
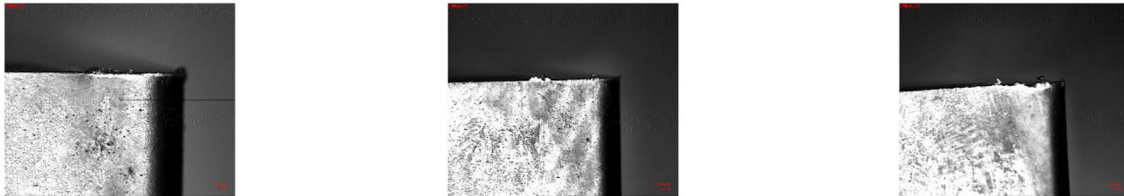
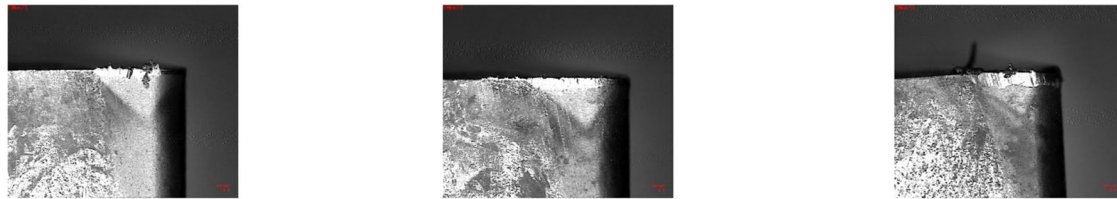
(a) AlTiN**(b) AlCrN****(c) Uncoated**

Fig. 16 Microscopic images showing flank wear progression for **a** AlTiN, **b** AlCrN and **c** uncoated inserts

workpieces with different cutting inserts revealed that the AlTiN-coated insert exhibited most appropriate surface finish with lowest surface roughness value. The surface roughness values attained for AlCrN coating displayed comparable levels of R_a value. The AlTiN-coated inserts have better self-organising capabilities and can adapt to external stimuli much better than AlCrN-coated inserts at 10 m/min. During the cutting process, a part of the energy is consumed during the self-organisation [51] of the coating that forms a lubricating tribo-layer responsible for reducing the friction at chip–tool interface and therefore better tool life.

Theoretically, adhesive wear is expected to predominantly manifest in lower to medium cutting speed, since at high cutting speed, the chips have very little contact time to adhere. As expected, while investigating tool life at a higher cutting speed of 140 m/min, we observed that AlTiN-coated inserts performed marginally better than AlCrN-coated inserts. The evolution of flank wear with time for both the coated inserts was observed to be gradual and consistent for majority of the machining time, but as the machining progressed, a sudden acceleration in flank wear was noted. The presence of Cr in AlCrN coatings should ideally improve the plasticity of

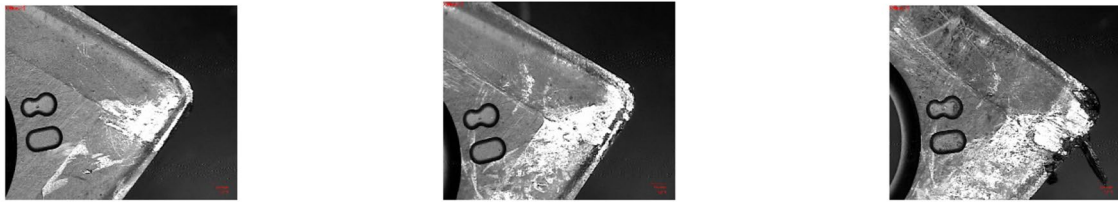
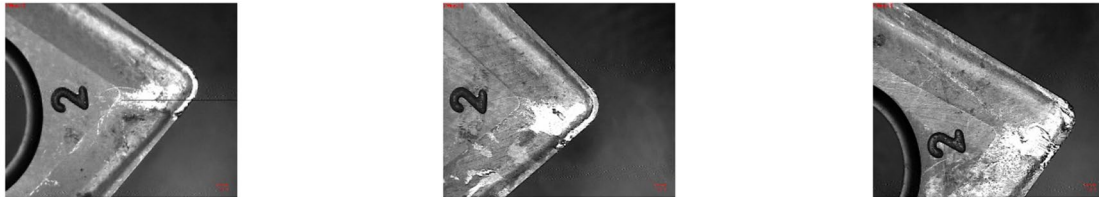
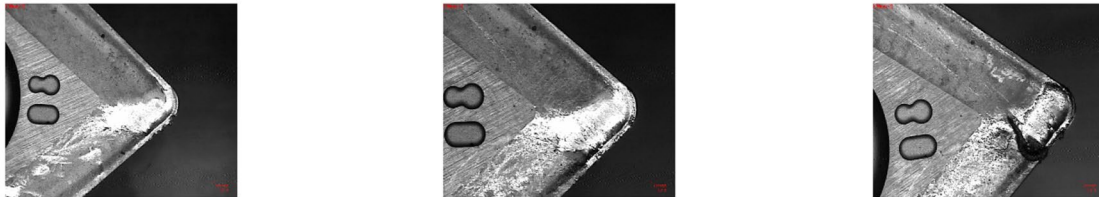
(a) AlTiN**(b) AlCrN****(c) Uncoated**

Fig. 17 Microscopic images showing crater wear progression for **a** AlTiN, **b** AlCrN and **c** uncoated inserts

the coating and hence better performance under severe wear conditions. This is evident from the fact that the crater wear in AlCrN-coated inserts is not that significant as is seen in AlTiN-coated inserts. There are studies that show the superior tribological performance of AlCrN-coated inserts over AlTiN inserts when it comes to high-speed machining. While our study is focused on low to moderate cutting speeds, the scope for investigation at high cutting speeds in excess of 200 m/min, high feed and light cuts exists.

Compliance with ethical standards

Conflict of interest The author(s) declare that they have no competing interests.

References

- Gamarra JR, Anselmo ED (2018) Taper turning of super duplex stainless steel: tool life, tool wear and workpiece surface roughness. *J Braz Soc Mech Sci Eng*. <https://doi.org/10.1007/s40430-018-0991-1>
- Paro J, Hänniken H, Kaupinen V (2001) Tool wear and machinability of HIPed P/M and conventional cast duplex stainless steels. *Wear* 249:279–284
- Oliveira Junior CA, Diniz AE, Bertazzoli R (2014) Correlating tool wear, surface roughness and corrosion resistance in the turning process of super duplex stainless steel. *J Braz Soc Mech Sci Eng* 36:775–785. <https://doi.org/10.1007/s40430-013-0119-6>
- Yassmin SA, Jose MP, Covelli Danielle, Stephen CV (2017) Investigation of coated cutting tool performance during machining of super duplex stainless steels through 3D wear evaluations. *Coatings* 7:127. <https://doi.org/10.3390/coatings7080127>
- Dogra M, Sharma VS (2012) Machinability and surface quality issues in finish turning of hardened steel with coated carbide and CBN tools. *Mater Manuf Process* 27(10):1110–1117. <https://doi.org/10.1080/10426914.2011.654164>
- Wong YS, Nee AYC, Li XQ, Riesdorf C (1997) Tool condition monitoring using laser scatter pattern. *J Mater Process Technol* 63:205–210. [https://doi.org/10.1016/s0924-0136\(96\)02625-8](https://doi.org/10.1016/s0924-0136(96)02625-8)
- Bradley C, Wong YS (2001) Surface texture indicator of tool wear—a machine vision approach. *Int J Adv Manuf Technol* 17:435–443. <https://doi.org/10.1007/s001700170161>
- Choudhury SK, Bartarya G (2003) Role of temperature and surface finish in predicting tool wear using neural network and design of experiments. *Int J Mach Tools Manuf* 43:747–753. [https://doi.org/10.1016/s0890-6955\(02\)00166-9](https://doi.org/10.1016/s0890-6955(02)00166-9)
- Ozel T, Karpat Y, Figueira L, Paulo Davim J (2007) Modelling of surface finish and tool flank wear in turning of AISI D2 steel with ceramic wiper inserts. *J Mater Process Technol* 189:192–198. <https://doi.org/10.1016/j.jmatprotec.2007.01.021>

10. ISO 3685 (1993) Tool-life testing with single-point turning tools. International Organization for Standardization. <https://www.iso.org/standard/9151.html>
11. Nomani J, Pramanik A, Hilditch T (2013) Machinability study of first generation duplex (2205), second generation duplex (2507) and austenite stainless steel during drilling process. *Wear* 304:20–28
12. Dureja JS, Gupta VK, Sharma VS, Dogra M (2009) Wear mechanisms of TiN-coated CBN tool during finish hard turning of hot tool die steel. *Proc Inst Mech Eng Part B J Eng Manuf* 224(4):553–566. <https://doi.org/10.1243/09544054jem1664>
13. Selvaraj DP, Chandramohan P, Mohanraj M (2014) Optimization of surface roughness, cutting force and tool wear of nitrogen alloyed duplex stainless steel in a dry turning process using Taguchi method. *Measurement* 49:205–215
14. Krolczyk G, Legutko S, Gajek M (2013) Predicting the surface roughness in the dry machining of duplex stainless steel DSS. *Metalurgija* 52:259–262
15. Jawaid A, Olajire K, Ezugwu O (2001) Machining of martensitic stainless steels (JETHETE) with coated carbides. *Proc Inst Mech Eng Part B J Eng Manuf* 215:769–779
16. Nomani J, Pramanik A, Hilditch A, Littlefair G (2015) Chip formation mechanism and machinability of wrought duplex stainless steel alloys. *Int J Adv Manuf Technol* 80(5–8):1127–1135
17. Ahmed YS, Paiva JM, Bose B, Veldhuis SC (2019) New observations on built-up edge structures for improving machining performance during the cutting of superduplex stainless steel. *Tribol Int.* <https://doi.org/10.1016/j.triboint.2019.04.039>
18. Trent EM, Wright PK (2000) *Metal cutting*, 4th edn. Butterworth-Heinemann, Woburn
19. Boothroyd G, Knight WA (2006) *Fundamentals of machining and machine tools*, 3rd edn. Taylor & Francis Group, Abingdon-on-Thames
20. Yassmin SA, Stephen CV (2017) The study of wear performance and chip formation of coated carbide tools during machining super duplex stainless steels. In: Conference: VMPT
21. Paiva JM, Torres RD, Amorim FL, Covelli D, Tauhiduzzaman M, Veldhuis SC, Dosbaeva G, Fox-Rabinovich (2017) Frictional and wear performance of hard coatings during machining of super duplex stainless steel. *Int J Adv Manuf Technol* 24:1–10
22. Prakash L (2014) *Fundamentals and general applications of hardmetals*. Elsevier, Amsterdam
23. Viktor PA, Davim J (2008) *Tools (geometry and material) and tool wear*. In: *Machining*. Springer, London. https://doi.org/10.1007/978-1-84800-213-5_2
24. Davim JP (2008) *Machining*. Springer, Berlin
25. Soković M (2007) Quality management in development of hard coatings on cutting tools. *J Achiev Mater Manuf Eng* 24(1):421
26. Dobrzański LA, Lukaszewicz K, Labisz K (2009) Structure, texture and chemical composition of coatings deposited by PVD techniques. *Arch Mater Sci Eng* 37(1):45
27. Aslan E (2005) Experimental investigation of cutting tool performance in high speed cutting of hardened X210 Cr12 cold-work tool steel. *Mater Des* 26:21–27
28. Minevich AA (1992) Wear of cemented carbide cutting inserts with multilayer Ti-based PVD coatings. *Surf Coat Technol* 53:161–170
29. Audy Strafford J, Subramanian KN (1995) The efficiency of uncoated and coated tool systems in the machining of low carbon steel assessed through cutting force measurements. *Surf Coat Technol* 76–77:706–711
30. Minevich AA, LA Eizner Crick, Popok (2000) Case studies on tribological behaviour of coated cutting tools. *Tribol Trans* 43(4):740–748
31. Sampath Kumar T, Balasivanandha Prabu S, Manivasagam Geetha, Padmanabhan KA (2014) Comparison of TiAlN, AlCrN, and AlCrN/TiAlN coatings for cutting-tool applications. *Int J Miner Metall Mater* 21:796. <https://doi.org/10.1007/s12613-014-0973-y>
32. Mrkvica I, Petru J, Slehal V, Neslusan M, Jurko J, Panda A (2015) Properties of cutting inserts with different PVD coatings. *MM Sci J* 2015(2):600603. https://doi.org/10.17973/MMSJ.2015_06_201501
33. *Handbook of stainless steels*, Outokumpu Oyj, Finland, 2013. <https://fliphtml5.com/jjnr/nqfb>
34. Nilsson JO, Karlsson L, Andersson JO (1995) Secondary austenite formation and its relation to pitting corrosion in duplex stainless-steel weld metal. *Mater Sci Technol* 11:276–283
35. *Practical Guidelines for the fabrication of Duplex Stainless Steels*. 2nd Edn. (2009) International Molybdenum Association, London, UK, ISBN 978-1-907470-00-4
36. Rastee DK, Siegfried Schmauder, Eisseler R (2013). Machining of stainless steels: a comparative study. In: International conference on advanced manufacturing engineering and technologies
37. Sargade VG, Gangopadhyay S, Paul S, Chattopadhyay AK (2011) Effect of coating thickness on the characteristics and dry machining performance of TiN film deposited on cemented carbide inserts using CFUBMS. *Mater Manuf Process.* <https://doi.org/10.1080/10426914.2010.526978>
38. Coromant Sandvik (2009) *Catálogo principal*. AB Sandvik Coromant, Sandviken, pp A424–A433
39. Subhash N, Sambadana S, Nithin Raj P, Jagadeesha T (2019) Experimental study on tool wear and optimization of process parameters using ANN-GA in turning of super-duplex stainless steel under dry and wet conditions. *Adv Manuf Technol.* https://doi.org/10.1007/978-981-13-6374-0_47
40. Korkut I, Kasap M, Ciftci I, Seker U (2004) Determination of optimum cutting parameters during machining of AISI 304 austenitic stainless steel. *Mater Des* 25(4):303–305. <https://doi.org/10.1016/j.matdes.2003.10.011>
41. Shaw M (2005) *Metal cutting principles*, 2nd edn. Oxford University Press, New York
42. Jacobson S, Hogmark (2010) Tribofilms—On the crucial importance of tribologically induced surface modification. In: Nikas GK (ed) *Recent developments in wear prevention, friction and lubrication*. Research Signpost, Kerala
43. Fox-Rabinovich GT (2006) *Self-organization during friction: advanced surface-engineered materials and systems design*. CRC Press, Boca Raton
44. Mo JL, Zhu MH, Leyland A, Matthews A (2013) Impact wear and abrasion resistance of CrN, AlCrN and AlTiN PVD coatings. *Surf Coat Technol* 215:170–177
45. Corrêa JG, Schroeter RB, Machado AR (2017) Tool life and wear mechanism analysis of carbide tools used in the machining of martensitic and supermartensitic stainless steels. *Tribol Int* 105:102–117
46. Junior AB, Diniz AE, Teixeira Filho F (2009) Tool wear and tool life in end milling of 15–5 PH stainless steel under different cooling and lubrication conditions. *Int J Adv Manuf Technol* 43:756–764
47. *ASTM G40-15—Standard Terminology Relating to Wear and Erosion*. ASTM: West Conshohocken, PA, USA (1987); Vol. 03.02, pp. 243–250
48. Melo AC, Milan JCG, Silva MB, Machado AR (2006) Some observations on wear and damage in cemented carbide tools. *J Braz Soc Mech Sci Eng* 28:269–277
49. Noordin MY, Venkatesh VC, Sharif S (2007) Dry turning of tempered martensitic stainless tool steel using coated cermet and coated carbide tools. *J Mater Proc Technol* 185:83–90
50. Raof NA, Ghani JA, Syarif J, Che Hassan CH, Hadi MA (2014) Comparison of dry and cryogenic machining on chip formation and coefficient of friction in turning AISI 4340 alloy steel. *Appl Mech Mater* 554:7–11

51. Ahmed YS, Jose MP, Covelli D, Veldhuis SC (2017) Investigation of coated cutting tool performance during machining of super duplex stainless steels through 3D wear evaluations. *Coatings* 7:1–15. <https://doi.org/10.3390/coatings7080127>
52. Complete Machining Solutions (2017) Rotating Tool Lines, Metric Version Catalog, ISCAR
53. Nilsson JO (1992) Super duplex stainless steels. *Mater Sci Technol* 8:685–700

Publisher's Note Springer Nature remains neutral with regard to jurisdictional claims in published maps and institutional affiliations.